Determining the Lipid Specificity of Insoluble Protein Transmembrane Domains

Journal:	*Lab on a Chip*
Manuscript ID	LC-ART-03-2018-000311.R2
Article Type:	Paper
Date Submitted by the Author:	07-Oct-2018
Complete List of Authors:	Ziblat, Roy; Harvard University, School of Engineering and Applied Sciences Weaver, James; Wyss Institute, Arriaga, Laura; Universidad Complutense de Madrid, Department of Physical Chemistry I Chong, Shaorong; New England Biolabs Inc Weitz, David; Harvard University, Department of Physics

Determining the Lipid Specificity of Insoluble Protein Transmembrane Domains

R. Ziblat[*1], J.C. Weaver[2], L.R. Arriaga[3], S. Chong[4], D.A. Weitz*[*1,5]*

[1]School of Engineering and Applied Sciences, Harvard University, Cambridge, MA 02138, USA

[2]Wyss Institute for Biologically Inspired Engineering, Harvard University, Cambridge, MA 02138, USA

[3]Department of Physical Chemistry, Universidad Complutense, Madrid, 28040, Spain.

[4]New England Biolabs, Inc. 240 County Road, Ipswich, MA 01938, USA

[5]Department of Physics, Harvard University, Cambridge, MA02138, USA

Keywords: Lipid Membranes, Transmembrane Domains, Protein-Lipid Specificity, Liposome Library, Microfluidics

Abstract

While the specificity of protein-lipid interactions is a key feature in the function of biological membranes, studying the specifics of these interactions is challenging because most membrane proteins are insoluble in water due to the hydrophobic nature of their transmembrane domains (TMDs). Here, we introduce a method that overcomes this solubility limitation and identifies the affinity profile of protein TMDs to specific lipid formulations. Using 5 human TMDs as a sample group, our results demonstrate that TMDs are highly selective and that these specific lipid-TMD interactions depend not only on the presence of a single lipid, but on a combination of a few lipids.

Introduction

In most species, about a quarter of the genes encode for membrane proteins.(1) These proteins participate in many cellular processes on the membrane, and the unique protein composition determines the structure and function of each membrane type.(2-5) Membranes also differ in the variety of lipids that compose them, and there is a strong correlation between protein and lipid composition.(6-8) Membrane proteins are anchored to the lipids by their hydrophobic Transmembrane Domains (TMDs), which span through the lipid bilayer. The hydrophobic TMDs can be lipid specific, suggesting that TMD specificity to the composition of the local lipid environment is a key component in membrane architecture.(9, 10) TMDs can, therefore, serve as a good model system for studying the specificity of protein-lipid interactions. Studying TMD-lipid specificity is challenging, however, because the TMDs are water insoluble, and any detergents used to solubilize the hydrophobic TMDs would get incorporated in a non-specific manner into the membrane and alter its structure. Nevertheless, determining the specificity of TMDs to lipids is essential to our basic understanding of membrane function, and may be an important step for designing drugs that target specific cell membranes or tissues. While the identification of lipids to which each TMD is in contact is essential for structural studies of membrane proteins(8, 11, 12), current crystallization attempts and *in vitro* or *in silico* studies of membrane proteins are usually performed without prior knowledge of the lipid environment each protein requires. There is, therefore, a need to overcome the solubility limitation of TMDs for the identification of these lipid-specific interactions.

In the present study, we present a methodology to identify the lipid compositions that TMDs require for membrane incorporation. We show that these specific TMD-lipid interactions can depend on either the presence of a single lipid, or the combined effect of multiple lipid species. To determine the TMD-lipid specificity, a membrane library that contained the major classes of cellular lipids (13-15) was created and incorporated into a microfluidic device. To overcome the bulk TMD solubility problem, fluorescently tagged TMD constructs (with GFP) were locally synthesized using a reconstituted cell-free protein synthesis system, via *in-vitro* Transcription and Translation (IVTT) (16-18) within the microfluidic channels, and in close proximity to the lipid membranes. Depending on the lipid composition, each TMD molecule could, in turn, either bind to and become directly incorporated into the lipid membrane, or remain excluded from the

membrane and form TMD aggregates in solution (19). In the present study, we used this approach to investigate the lipid-binding specificity of TMDs from five human proteins.

Results

Experimental

Lipid library: A membrane library was created for studying the specificity of TMDs to different lipid compositions. To test whether this specificity was a function of one or more lipids, the membranes that constituted the library were composed of either a single or a combination of different lipid types. The library contained 120 different formulations, composed of lipids from both dominant cell membrane lipid classes, the sphingolipids and the glycerolipids. These classes were further separated into sub-groups of saturated and unsaturated lipids. Since there was little prior knowledge of the types of lipids that were in contact with a protein's binding site, the library included the probable combinations of these groups according to known average membrane lipid compositions (20). This library design was chosen in an attempt to replicate possible lipid compositions that surround the different TMDs as they span through the membranes of different cell types. All lipid formulations consisted of at least 55% unsaturated species to facilitate spontaneous swelling of the lipid films into free floating membranes. In addition, all lipid formulations included cholesterol ,a member of the sterol class, which is a common component of all membranes in human cells.(21) The lipid types that composed the library and the detailed lipid composition of the full library are described in Table 1 and Supplementary Table 1, respectively. The considerations for including each lipid specie in the library are as follow; While the average lipid composition of each cell organelle is known, there is limited knowledge of the local composition at the binding site of TMD-containing proteins. As a result, choosing which lipids to include in the library was challenging. Most of the commercially available lipids (Avanti Lipids) used in this study were cell extracted and therefore contained a mixture of lipids that exhibited variability in chain length and degree of saturation. The benefits of using such reagents are that they increase the probability that the required lipid combinations for each TMD is present in the lipid library. PC, PE, Sphingomyelin, Ganglioside, Cerebroside, Ceramide, and PS lipid products were chosen for their high abundancy in different cell and organelle membranes, while BMP lipid is highly abundant in the late endosome organelle. PA, PI and PG are also found in significant

quantities, and since many biochemical interactions rely on the molecular charge, we also examined the dependency of binding specificity on the presence of charged lipids. While DGPP is not particularly abundant in cells, it does have a double charge, and here we investigated this property on TMD binding affinity. Ceramide is a precursor of sphingolipids, and as such has been found to be important for protein sorting and cell function. DAG has the same hydroxyl headgroup as Ceramide and the affinities of Ceramide and DAG are also compared. Lastly, most lipids have two fatty acid chains, and so to examine the role of double chain versus single chain lipids, we included N-palmitoylglycine and Lyso PC (which each have a single chain). For the complete list of lipid products, see Supplementary Table 2.

All 120 lipid mixtures were made, dissolved in chloroform at 2 mg/mL, stored in glass vials at -20°C, and each well in the microfluidic device was seeded with approximately 5 μL of these lipid solutions. The recombinant Alexa Fluor® 488-conjugated Cholera toxin subunit B was obtained from Thermo Fischer Scientific - Life Technologies. The reconstituted cell-free system (IVTT) was the PURExpress system (New England Biolabs). The water used for third confocal scan, following the binding measurement, performed to visualize liposomes and compare flows to each well, was dyed using 0.1 g/L sulforhodamine B (Sigma).

Microfluidic device: Polydimethylsiloxane (PDMS) microfluidic devices were fabricated using standard soft lithography methods (22) and consisted of a multi-well format (9×12 wells), where each well was seeded with a different lipid formulation. Outflow from each well led directly to the outlet of the device and did not pass through other wells to avoid lipid cross-contamination between wells. The heights of the inlet channels, wells, and outlet channels were 15 μm, 50 μm, and 75 μm respectively; this design created high resistance in the inlets and low resistance at the outlets, which prevented undesired backflow from adjacent wells through the outlet channels. Each well included PDMS posts with square cross-sections to increase the surface area for liposome swelling and provided a physical barrier for liposome immobilization. Solutions and reagents were introduced through source inlets that distributed equal volumes of solutions throughout all of the micro-wells.

Prior to bonding of the PDMS microchannels to a second flat plasma-treated PDMS sheet, ca. 5 μg of lipids from the lipid library were deposited into each of the microfluidic wells using a

glass capillary brush. The lipid solutions were added to a chloroform-based solvent which evaporated within a few seconds, leaving dry lipid films. To expedite the experimental set up and to minimize environmental contamination, the capillary brush was designed to collect 12 different lipid formulations at a time. This process was repeated 9 times for deposition into all 108 wells, and the PDMS channels were then bonded with a second PDMS layer to form the closed microfluidic device (Supplementary figure 1). The microfluidic device with the dried lipid films was stored under vacuum. For the affinity experiments, this device was filled with de-gassed milli-Q (Millli-pore filtered) water and placed in a 65°C oven for 1 hour to facilitate into liposomes (spherical membranes). The total volume of the microfluidic chip, channels and wells, was less than 40 μL, requiring minute volumes of lipids and cell-free IVTT reagents, as compared to those used in traditional multi-well plate-based set ups. (Figure 1)

Imaging: Experimental data were collected as a z-stack of images from all wells on the device using a confocal microscope (Leica TSC SP5) equipped with a 10× air objective (numerical aperture of 0.3), and bright field and fluorescence images were sequentially acquired at each experimental time point. To measure the bound GFP signal, we used an argon (488 nm) laser as an excitation source and fluorescence emission was collected by a photomultiplier tube through a bandpass filter between 525 and 570 nm. All xyz scans were performed at room temperature at a z-slice step size of 7μm. Scans were performed three times per experiment, with the first scan as a control after liposome swelling, but prior to TMD embedding. After the fluorescent GFP-labeled TMDs were introduced to the membranes, the wells were flushed with 40 times their volume of milli-Q water to exclude unbound proteins, and then second scan was performed. For the third scan, the wells were filled with sulforhodamine-dyed water (100 mg/L) to measure the flow that passed through each well. While the wells were designed to have equal flow, differential liposome dwelling could restrict flow and thus lead to uneven flow over the course of the experiment. The third scan allowed, if necessary, compensation by normalizing the fluorescence data from wells with flow variances. The use of sulforhodamine-dyed water was also beneficial for detecting low light scattering uni-lamellar liposomes that were difficult to detect by transmitted light microscopy. (Supplementary figure 2, Video 1)

The liposome swelling processes in this study were highly variable and resulted in multi-lamellar membranes of different sizes. While there are alternative methods for liposome production, which can lead to a more uniform size distribution of uni-lamellar liposomes, working

with the multi-lamellar liposomes offered an advantage as these liposomes have proven to be more robust and able to withstand exposure to varying environments, including those required by the IVTT reagents. In contrast, attempts to repeat these experiments using giant uni-lamellar liposomes (23) with similar formulations were difficult because of their fragility, which resulted in liposome collapse during protein synthesis.

Image processing: Large liposomes with sizes above 10 μm were identified by image processing of either the transmitted light images or the negative images of the sulforhodamine-dyed water, which could reveal liposomes unrecognized in the transmittance images, (Supplementary figure 2). Once identified, the estimated surface areas of the liposomes were used to normalize the fluorescence signals. Fluorescence signals originating from smaller liposomes or tubular micelles, which were too small to be identified during image processing, were normalized by the number of fluorescent pixels in each of the image stacks. Each experiment was reproduced 3 to 5 times, and after image processing, the standard deviation for each well was 15-35% of its mean value. Control scans of the liposome library, performed prior to the introduction of the GFP-labeled TMDs, were subtracted from the scans performed with the TMDs, and then normalized to the volume of sulforhodamine-dyed water that flowed through each well (Supplementary figure 1). In some cases, non-specific labeling of the PDMS surfaces occurred, and so to eliminate these false-positives, PDMS surfaces of the wells and posts were identified through image processing, and any overlapping fluorescence originating from PDMS surfaces was subtracted.

To evaluate the performance of the microfluidic setup, we measured the liposome selectivity profile of Cholera Toxin subunit B (CTb). CTb is one of the few proteins whose selectivity for lipids is well characterized (24), and unlike TMDs, toxins such as CTb easily solubilize in aqueous solutions and are therefore ideal for membrane labeling experiments. Previous studies have shown that CTb co-purifies with ganglioside (GM1) lipids from cell cultures (25), demonstrating a strong affinity between these two molecules. CTb has since been widely used for GM1 labeling in cells, and here, we use 0.1 μM of fluorescently labeled CTb to evaluate the efficacy of our microfluidic device and the composition of its liposome library. Data obtained from the resulting confocal microscopy measurements were analyzed with custom image processing software designed in MatLab. Using this software, and as described above, fluorescence originating from PDMS

surfaces, which may have non-specifically labeled, was identified and subtracted. The results from this affinity control study clearly demonstrated that the CTb labeled all the liposomes containing GM1, and that there was negligible signal from wells with liposomes lacking GM1 (Figures 2 and 3). A summarizing video of the experimental setup is available in online (Video 1).

Transmembrane Domains

Historically, protein-lipid binding specificity has been generally attributed to the hydrophilic and chemically complex lipid headgroup, as the contribution of the length and saturation variation in the fatty acid chains has seemed minor, by comparison. Nevertheless, X-ray diffraction studies of model membranes have revealed that the hydrophobic cores can be structurally ordered, with strong dependence on the organization of the lipid fatty acid chains (26-29). To add complexity to this story, studies on human transmembrane emp24 domain-containing protein 2 (P24), which has a single α-helix spanning through the membrane, demonstrated lipid specificity to sphingomyelin (SM), even though the TMD was mostly in contact with the fatty acid chains. In comparison, the human transmembrane emp23 domain-containing protein 10 (P23) does not show affinity to SM.(10) However, for this protein, its single α -helix is in contact with more than one lipid molecule, suggesting that TMD specificity to membranes may not only depend on the presence of a single lipid but on a combination of multiple lipid species. Together, these observations illustrate the complexity of protein-lipid interactions and suggest that both head group and fatty acid chain chemistries likely play key roles in this observed specificity. To test the potential specificity of TMDs to an ensemble of multiple lipid species, we investigated the binding selectivity profiles of the TMDs of P24 and P23 to our liposome library.

In contrast to our CTb studies, the hydrophobic TMDs can frequently aggregate in aqueous solution, and as a result, binding studies on these TMDs could not simply be performed by injecting them directly into our microfluidic device. Instead, to measure TMD-lipid binding profiles in an aqueous environment, a synthetic protein consisting of each TMD fused to green fluorescent protein (GFP) was constructed. The GFP-TMD fusion proteins were produced through a reconstituted cell-free protein synthesis system, *via in-vitro* Transcription and Translation (IVTT) (16). Once the lipid films swelled into liposomes, the microfluidic device was filled with the IVTT reagents along with DNA that encoded for each of the GFP-TMD constructs, and protein synthesis was initiated by incubating the microfluidic device at 37°C for 2-3 hours (17). Under these

conditions, the GFP-TMDs were expressed in the vicinity of the liposomes and either embeded into the lipid membrane, or aggregated with other GFP-TMDs to form micelles (30). Following initial incubation, the non-bound aggregates of GFP-TMDs were washed away by passing a constant flow of water through the microfluidic device.

Comparison of the affinity profiles of P23 and P24 confirmed that P24 bound well to SM-containing lipid formulations, whereas P23 did not (Fig SI, Table1). P24 binding was, however, dependent on the presence of additional lipid species comprising the liposomes. For example, it exhibited a strong affinity to SM:DAG:cholesterol and SM:cer:cholesterol, yet demonstrated negligible binding to the parts of these compositions, SM:cholesterol, DAG:cholesterol, and Cer:cholesterol. The results from these binding studies suggest that the affinity of P24 is a function of a combination of different lipid species. The highest P24 binding to SM-containing lipid formulations were for those that included Lyso-PC, DAG, Cermide and Cerebroside. While the SM used in the library was composed mostly of chain length SM 16:0, it also included SM 18:0, to which P24 was found previously to bind (10). Notably, P24 also exhibited high affinities to additional lipid formulations that did not include SM, highlighting the complexity of these interactions. The relative affinity values of selected formulations are shown in Table 2, and the full profiles are available in the Supplementary Materials, Table 1.

In our microfluidic assay, the TMDs of tumor necrosis factor receptor superfamily member 5 (CD40) and receptor type tyrosine-protein phosphatase C (CD45) also exhibited lipid specificity. Previously, it has been shown that the TMD of the CD40 membrane protein was selective to specific lipid domains, which were mainly composed of cholesterol and sphingolipids (5). Comparison of the affinity profiles of the CD40 and CD45 TMDs obtained from our present study demonstrated that although the two exhibited some general trends (e.g. lipid formulations that exhibited >20% labeling included some type of sphingolipid) and did share affinities for a few lipid formulations, generally, each TMD exhibited a distinct affinity profile. (Figure 4 and Supplementary Materials, Table 1).

In contrast to the binding profiles of P23, P24, CD40, and CD45, the TMD of programmed cell death protein1 (PD1) was not lipid-specific. The affinity profile of PD1 showed significant labeling of most lipid formulations, where 40% of all liposomes in our library exhibited labeling intensities of over 25%, and 70% of the library had labeling intensities above 10%. This high

affinity to most liposomes was observed despite the fact that competitor TMDs were used in this study; specificity studies (26), unlike affinity studies, utilize non-labeled molecules to compete with the molecule of interest for the available binding sites (competitors thus reduce labeling of non-specific sites, to which a target molecule may have limited affinity). Here, competitor TMDs were used to eliminate binding of the GFP-TMD to low affinity lipids. In all of the TMD experiments, we used SNAP-TMDs with varying sequences of TMDs as competitors. SNAP (31) was chosen since it is a non-fluorescent protein, with a similar size as the GFP protein, and hence, was expected to be expressed at similar levels as the GFP-TMD constructs. The competitor addition was performed by including SNAP-TMD DNA along with the GFP-TMD DNA with the IVTT reagents. To favor the competitor, the ratio between the SNAP-TMD and GFP-TMD DNAs was 2:1. The competitors used in each experiment are detailed in the affinity Table 2 and Supplementary Materials, Table 1.

It should be noted that the IVTT reagents used in our approach contain many proteins and other biological molecules necessary for the expression of TMDs, which could have also interacted to some degree with the various components of our lipid library. Despite this possibility, considering the fact that the same IVTT reagents were used in all of the experiment and that each TMD exhibited a unique lipid-binding profile, it is unlikely that the IVTT reagents resulted in a significant number of false positive signals. In addition, very few lipid formulations exhibited negligible binding signals for all TMDs, suggesting that the IVTT reagents did not likely result in an appreciable number of false negatives, either. Nevertheless, it is possible that the use of different cell-free expression reagents could potentially influence the observed affinity profiles, and as such, future research aimed at optimizing the approach presented here should include such parallel studies.

To demonstrate the necessity of our experimental approach, a series of validation experiments were also preformed. For example, when GFP-TMDs were expressed in the absence of the liposome library, the proteins aggregated. When these aggregates were added back to the liposome library, a negligible amount of membrane fluorescence was detected, demonstrating that GFP-TMD aggregation prevented subsequent membrane incorporation. In addition, the liposome fluorescence measured in our experiments remained unchanged for at least 6 hours, indicating that once incorporated into the lipid membrane, the GFP-TMDs remained incorporated and were unlikely to equilibrate with the bulk solution during the subsequent washing stages. These results

therefore demonstrate that our IVTT approach is required for the expression of the GFP-TMD constructs in the vicinity of the membrane for investigating free TMD-lipid interactions.

To determine whether the liposome-bound TMDs remained inclined on the lipid surface or embedded in the membrane, a protease protection assay was employed (32). Liposomes composed of SM:DAG:cholesterol and SM:Cer:cholesterol, detailed in Table 2, were prepared in a tube, along with the IVTT reagents for expression the PD1, P24, and P23 GFP-TMDs. After membrane insertion of the TMDs, proteinase K was added, which degraded all exposed proteins, including the linked GFP; the proteinase cannot access peptides, which are embedded in the membrane. (Supplementary figure 3) Mass spectrometry analysis of these samples revealed 17-20 amino acid long peptides belonging to the PD1 and P24 TMDs, demonstrating that these peptides were in fact embedded in the hydrophobic cores of the membranes. In contrast, no peptides belonging to P23 were detected by mass spectrometry, demonstrating that the p23 TMD was not membrane-embedded, as suggested from the P23 affinity profiles in Table 2 and Supplementary Materials, Table 1.

Discussion

While diluted detergents are commonly used to embed insoluble proteins into lipid membranes (33), they can negatively affect the biochemistry of embedding, since the detergent molecules coat the proteins' hydrophobic lipid-binding sites. Because of these complications, the approach described here was developed as a detergent-free alternative for investigating the specificity of protein-lipid interactions.

It has been well established that lipids are not distributed homogeneously throughout the cell membrane, but rather are segregated into domains (34, 35) that have distinct lipid compositions. These domains (often called "lipid domains" or "lipid rafts") are hypothesized to be important for membrane function (3, 5) via their selective interaction with specific proteins. To investigate the nature of this specificity, a comprehensive lipid library was constructed. It should be noted, however, that these lipid formulations used in the present study were not an attempt to reproduce the domains or rafts that exist in specific cell types, nor the global average lipid composition of human cell membranes. Instead, the liposomes used in our study were chosen to

include structurally and chemically diverse lipid formulations for directly investigating the specificity of protein–lipid interactions and subsequent membrane incorporation. While the lipid compositions at the binding site of cell membrane proteins are currently unknown, the methodology introduced here is a first step toward providing an experimental toolkit for addressing such questions.

Several mechanisms have been proposed which partially explain the selective protein interactions with lipid membranes, which include specific affinities for lipid phases, membrane curvature, and membrane thickness (36, 37). The results shown here demonstrate that structural and chemical complementarities must also be considered and suggest that there could be a much larger variety of selective functional domains, since all five TMDs studied here show affinity for several different lipid formulations. It is thus likely that the TMD-lipid interactions detected here depend both on the affinity of the peptide to the lipid head-groups upon contact with the membrane followed by incorporation, and the thermodynamic preference to certain aliphatic chain environments, prolonging the TMD presence in the hydrophobic membrane core (38, 39). While our data cannot distinguish between these two mechanisms, it does provide experimental support to the hypothesis of lipid function by specificity to proteins and the importance of lipid diversity.

Approximately 60% of today's drugs target membrane proteins (40), yet surprisingly, we have limited tools to study the structure and local environment of these proteins. To address this largely unmet need, the liposome library described here can likely play a vital role in understanding the local lipid environment required for each protein. Identifying this protein-lipid specificity is essential for understanding protein transport in cells as well as for guiding simulation studies on membrane proteins, which are currently being performed without knowledge of the actual lipids for which they are in contact. This methodology may also serve as a tool for identifying the correct lipid composition to maintain protein structure and function, or for membrane protein crystallization studies. Lipid membranes have also been suggested to act as organic crystal nucleation sites (41), and our liposome library may help identify the best lipid composition for inducing or inhibiting such nucleation events. Just as the "druggable genome" concept includes all genes that are believed to interact with drugs (42), this methodology may lead to the identification of a "druggable lipids" framework, where all peptides will be indentified that interact with specific lipid compositions, and hence able to differentiate specific membranes, target specific organelles, cells, or species.

Acknowledgments

This study was supported by the Defense Advanced Research Projects Agency (HR0011-11-C-0093), the National Science Foundation (DMR-1310266), and by the Harvard Materials Research Science and Engineering Center (DMR-1420570). Microfluidic devices were prepared at the Center for Nanoscale Systems, at Harvard University. We are grateful for the support of Human Frontiers Science Program, Long Term Fellowship and to the Marie Curie International Outgoing Fellowship program within the EU Seventh Framework Programme for Research and Technological Development (2007-2013).

References

1. Krogh A, Larsson B, von Heijne G, & Sonnhammer ELL (2001) Predicting transmembrane protein topology with a hidden Markov model: Application to complete genomes. *J Mol Biol* 305(3):567-580.
2. Pagano RE & Sleight RG (1985) Defining Lipid Transport Pathways in Animal-Cells. *Science* 229(4718):1051-1057.
3. Simons K & Vanmeer G (1988) Lipid Sorting in Epithelial-Cells. *Biochemistry-Us* 27(17):6197-6202.
4. Obeid LM, Linardic CM, Karolak LA, & Hannun YA (1993) Programmed Cell-Death Induced by Ceramide. *Science* 259(5102):1769-1771.
5. Simons K & Ikonen E (1997) Functional rafts in cell membranes. *Nature* 387(6633):569-572.
6. Contreras FX, Ernst AM, Wieland F, & Brugger B (2011) Specificity of Intramembrane Protein-Lipid Interactions. *Csh Perspect Biol* 3(6).
7. Saliba AE*, et al.* (2014) A quantitative liposome microarray to systematically characterize protein-lipid interactions. *Nat Methods* 11(1):47-+.
8. Laganowsky A*, et al.* (2014) Membrane proteins bind lipids selectively to modulate their structure and function. *Nature* 510(7503):172-+.
9. Bock J & Gulbins E (2003) The transmembranous domain of CD40 determines CD40 partitioning into lipid rafts. *Febs Lett* 534(1-3):169-174.
10. Contreras FX*, et al.* (2012) Molecular recognition of a single sphingolipid species by a protein's transmembrane domain. *Nature* 481(7382):525-529.
11. Reichow SL & Gonen T (2009) Lipid-protein interactions probed by electron crystallography. *Curr Opin Struc Biol* 19(5):560-565.
12. Johansson LC, Wohri AB, Katona G, Engstrom S, & Neutze R (2009) Membrane protein crystallization from lipidic phases. *Curr Opin Struc Biol* 19(4):372-378.
13. Zaitseva E, Yang ST, Melikov K, Pourmal S, & Chernomordik LV (2010) Dengue Virus Ensures Its Fusion in Late Endosomes Using Compartment-Specific Lipids. *PLoS Pathog* 6(10).
14. Rimmerman N*, et al.* (2008) N-palmitoyl glycine, a novel endogenous lipid that acts as a modulator of calcium influx and nitric oxide production in sensory neurons. *Mol Pharmacol* 74(1):213-224.
15. van Schooten B, Testerink C, & Munnik T (2006) Signalling diacylglycerol pyrophosphate, a new phosphatidic acid metabolite. *Bba-Mol Cell Biol L* 1761(2):151-159.
16. Shimizu Y*, et al.* (2001) Cell-free translation reconstituted with purified components. *Nat Biotechnol* 19(8):751-755.
17. Shimizu Y, Kanamori T, & Ueda T (2005) Protein synthesis by pure translation systems. *Methods* 36(3):299-304.
18. Soga H*, et al.* (2014) In vitro membrane protein synthesis inside cell-sized vesicles reveals the dependence of membrane protein integration on vesicle volume. *ACS Synth Biol* 3(6):372-379.

19. Fujii S, Matsuura T, Sunami T, Kazuta Y, & Yomo T (2013) In vitro evolution of alpha-hemolysin using a liposome display. *Proc Natl Acad Sci U S A* 110(42):16796-16801.
20. van Meer G (2010) Membrane lipids, where they are and how they behave: Sphingolipids on the move. *Faseb J* 24.
21. van Meer G, Voelker DR, & Feigenson GW (2008) Membrane lipids: where they are and how they behave. *Nat Rev Mol Cell Bio* 9(2):112-124.
22. Qin D, Xia YN, & Whitesides GM (2010) Soft lithography for micro- and nanoscale patterning. *Nat Protoc* 5(3):491-502.
23. Wesolowska O, Michalak K, Maniewska J, & Hendrich AB (2009) Giant unilamellar vesicles - a perfect tool to visualize phase separation and lipid rafts in model systems. *Acta Biochim Pol* 56(1):33-39.
24. Zhang RG*, et al.* (1995) The 3-Dimensional Crystal-Structure of Cholera-Toxin. *J Mol Biol* 251(4):563-573.
25. Wiegandt H*, et al.* (1976) Studies of Ligand-Binding to Cholera Toxin .1. Lipophilic Moiety of Sialoglycolipids. *H-S Z Physiol Chem* 357(11):1637-1646.
26. Kuzmenko I*, et al.* (2001) Design and characterization at crystalline thin film architectures at the air-liquid interface: Simplicity to complexity. *Chem Rev* 101(6):1659-1696.
27. Ziblat R, Leiserowitz L, & Addadi L (2011) Crystalline Lipid Domains: Characterization by X-Ray Diffraction and their Relation to Biology. *Angew Chem Int Edit* 50(16):3620-3629.
28. Ege C, Ratajczak MK, Majewski J, Kjaer K, & Lee KYC (2006) Evidence for lipid/cholesterol ordering in model lipid membranes. *Biophys J* 91(1):L1-L3.
29. Brezesinski G*, et al.* (1995) Influence of Ether Linkages on the Structure of Double-Chain Phospholipid Monolayers. *Chem Phys Lipids* 76(2):145-157.
30. Goren MA, Nozawa A, Makino S, Wrobel RL, & Fox BG (2009) Cell-Free Translation of Integral Membrane Proteins into Unilamelar Liposomes. *Method Enzymol* 463:647-673.
31. Keppler A*, et al.* (2003) A general method for the covalent labeling of fusion proteins with small molecules in vivo. *Nat Biotechnol* 21(1):86-89.
32. Stefanovic S & Hegde RS (2007) Identification of a targeting factor for posttranslational membrane protein insertion into the ER. *Cell* 128(6):1147-1159.
33. le Maire M, Champeil P, & Moller JV (2000) Interaction of membrane proteins and lipids with solubilizing detergents. *Bba-Biomembranes* 1508(1-2):86-111.
34. Hancock JF (2006) Lipid rafts: contentious only from simplistic standpoints. *Nat Rev Mol Cell Bio* 7(6):456-462.
35. Veatch SL & Keller SL (2005) Miscibility phase diagrams of giant vesicles containing sphingomyelin. *Phys Rev Lett* 94(14).
36. Sprong H, van der Sluijs P, & van Meer G (2001) How proteins move lipids and lipids move proteins. *Nat Rev Mol Cell Bio* 2(7):504-513.
37. Andersen OS & Koeppe RE (2007) Bilayer thickness and membrane protein function: An energetic perspective. *Annu Rev Bioph Biom* 36:107-130.
38. Polyansky AA, Volynsky PE, Arseniev AS, & Efremov RG (2009) Adaptation of a membrane-active peptide to heterogeneous environment. II. The role of mosaic nature of the membrane surface. *J Phys Chem B* 113(4):1120-1126.

39. Pyrkova DV, Tarasova, N.K., Pyrkov, T.V., Krylov, N.A., Efremov, R.G. (2011) Atomic-scale lateral heterogeneity and dynamics of two-component lipid bilayers composed of saturated and unsaturated phosphatidylcholines. *Soft Matter* 7:2569-2579.
40. Overington JP, Al-Lazikani B, & Hopkins AL (2006) Opinion - How many drug targets are there? *Nat Rev Drug Discov* 5(12):993-996.
41. Kapishnikov S*, et al.* (2012) Oriented nucleation of hemozoin at the digestive vacuole membrane in Plasmodium falciparum. *P Natl Acad Sci USA* 109(28):11188-11193.
42. Hopkins AL & Groom CR (2002) The druggable genome. *Nat Rev Drug Discov* 1(9):727-730.

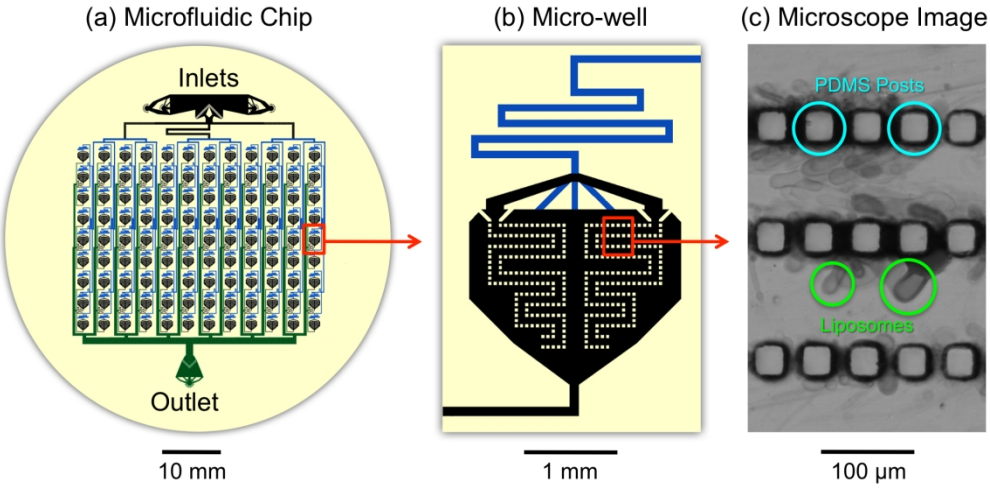

Details of the microfluidic device used in this study. (a) Schematics of the microfluidic device with 108 wells, each containing a different lipid formulation. Colors represent channel depth; Blue-15 µm, Black-50 µm, and Green-75 µm. (b) Enlarged schematic of a single well and (c) a corresponding photograph of the boxed region in (b) showing liposomes swelling off the surfaces of the square PDMS posts.

730x354mm (72 x 72 DPI)

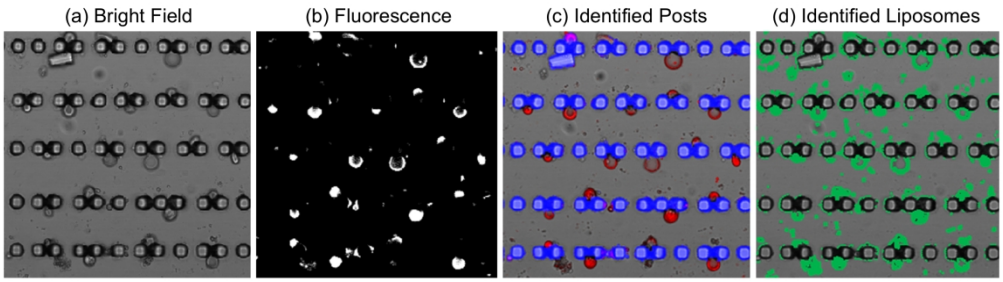

Confocal microscopy images of membrane labeling by fluorescently-tagged Cholera Toxin subunit B (CTb). (a) Brightfield image showing vesicles swelled on the surface of the square PDMS posts. (b) Fluorescence from the CTb. (c) Identification of PDMS surfaces (Blue) by image processing of (a) and fluorescence (Red) from image (b), and d) Identification of the liposomes (Green) by image processing of (c). All images measure 600 μm wide.

899x251mm (72 x 72 DPI)

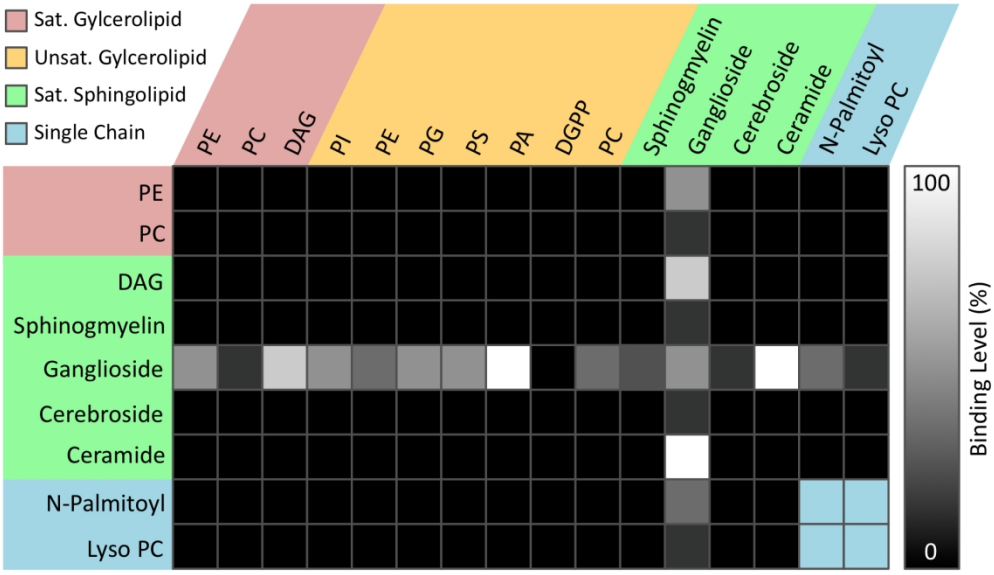

Cholera Toxin subunit B (CTb) specificity profile to the liposome library. Each square represents the relative fluorescence intensity as measured from each corresponding lipid formulation, and the lipids are divided to subgroups represented by colors. The brightness intensity scale (with the highest affinity normalized to 100%) represents the CTb's fluorescence per unit area found on the liposome surfaces. Lipid formulation ratios along with relative binding for each formulation can be found in Supplementary Table 1. The rational for choosing each lipid type is explained in the sub-section Lipid Library in the Experimental section. The results from this control screening demonstrate that CTb only binds to formulations containing ganglioside (GM1).

664x384mm (72 x 72 DPI)

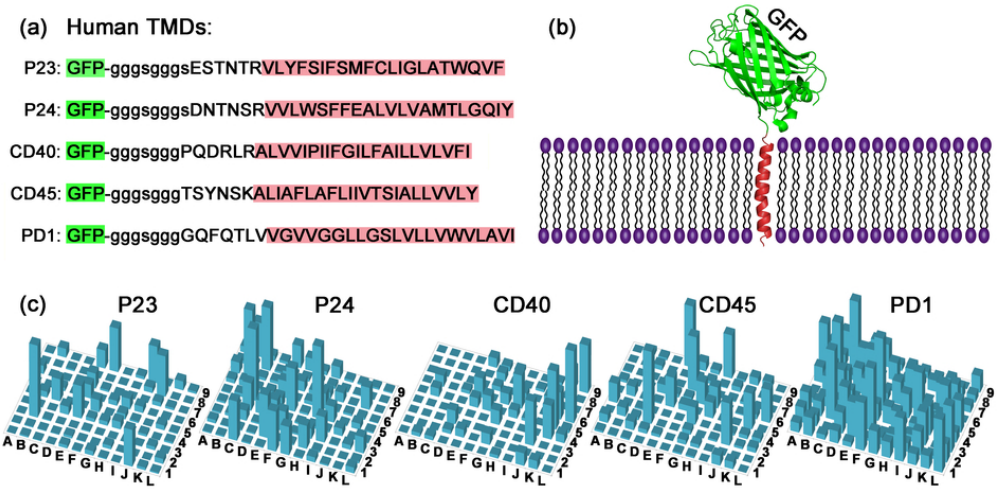

Affinity of human protein Transmembrane Domains (TMDs) to our liposome library. a) TMD peptide sequences used in this study. b) Schematic of a GFP-TMD embedded in a lipid bilayer. c) Affinity profiles of GFP-TMDs to the liposome library. Each of the matrices is normalized relatively to its highest fluorescence intensity. Positions of bars A-L and 1-8 correspond with the microfluidic matrix positions. The differences between the affinity profiles show the unique lipid specificity of each TMD.

80x39mm (300 x 300 DPI)

	Class	Lipid	Sat.	Unsat.	Unk.
Saturated	Glycerol	Hydro PC	99.3	0.7	0
		PE	56.6	43.4	0
		DAG	100	0	0
		Lyso PC	93.6	5.4	1
	Sphingo	Sphinogmyelin	69	21	10
		Ganglioside	100	0	0
		Cerebroside	49	9	42
		Ceramide	97	0	3
		N-Palmitoylglycine	100	0	0
Unsaturated	Glycerol	DGPP	0	100	0
		PC	18.6	80	1.2
		PE	20	78	2.2
		PG	20	70	10
		PS	13	87	0
		PI	38	62	0
		PA	45.7	54.3	0
		BMP (S,R) 18:1	0	100	0
		POPC	0	100	0
Sterol		Cholesterol	0	100	0

The lipid types in our membrane library. Due to their method of commercial production, most of the lipids listed here contained more than one structural varient, differing by either or both, the fatty acid chain length and degree of saturation as obtained from manufacturer. There are 67 different lipids in total, including glycerolipids, sphingolipids, and sterols. Lipid ratios of all liposomes in the library are detailed in Supplementary Table 1.

384x452mm (72 x 72 DPI)

Position		Lipid Group 1		Lipid Group 2		Lipid 3	Lipid 4	TMD	
								P24	P23
X	Y	Lipid Type	Mol. Ratio (%)	Lipid Type	Mol. Ratio (%)	Chol. (%)	POPC (%)	Competitors	
								P23 PD1	P24 PD1
C	8	SM	17	DAG	17	15	51	87	2
H	8	SM	29	PS	56	15		4	0
B	8	SM	24	PA	24	15	37	3	0
E	5	SM	17	NPG	17	15	51	14	1
E	2	SM	17	Cer	17	15	51	59	3
B	5	SM	38			15	47	5	8
K	5	SM	70			30		8	7
B	6	Cer	64			36		8	0
F	8	DAG	64			36		4	0

TMD affinity values to selected liposome formulations. Each of the TMD affinity values are normalized separately as a function of the highest value for that TMD. Values range from 0 to 100, and higher affinity values are highlighted in darker greens. Positions X and Y correspond to the location in the matrices as they appear in Figures 3 and 4. Since highly saturated lipid formulations are less likely to swell into liposomes, POPC was added to these formulations, as a representative phosphocholine lipid. All liposomes included cholesterol, because both phosphocholines and cholesterol are highly abundant in all human cell membranes.

618x413mm (72 x 72 DPI)

Overcoming solubility of membrane protein transmembrane domains to study their specificity to lipid compositions.